

Fluctuations, convergence times, correlation functions, and power laws from many-body Lyapunov spectra for soft and hard disks and spheres

Christoph Dellago

Department of Chemistry, University of Rochester, Rochester, New York 14627-0216

Wm. G. Hoover

Department of Applied Science, University of California at Davis/Livermore and Lawrence Livermore National Laboratory, Livermore, California 94551-7808

Harald A. Posch

Institute for Experimental Physics, University of Vienna, Boltzmannngasse 5, A-1090 Vienna, Austria

(Received 19 January 2002; published 20 May 2002)

The dynamical instability of many-body systems is best characterized through the time-dependent local Lyapunov spectrum $\{\lambda_j\}$, its associated comoving eigenvectors $\{\delta_j\}$, and the “global” time-averaged spectrum $\{\langle\lambda_j\rangle\}$. We study the *fluctuations* of the local spectra as well as the *convergence rates* and *correlation functions* associated with the δ vectors as functions of j and system size N . All the number dependences can be described by simple *power laws*. The various powers depend on the thermodynamic state and force law as well as system dimensionality.

DOI: 10.1103/PhysRevE.65.056216

PACS number(s): 05.45.-a, 05.20.-y

I. INTRODUCTION

Since dynamical instabilities are quantified by the time-dependent local Lyapunov exponents $\{\lambda_j\}$ [1,2] and because these quantities are, in favorable cases, simply related to the thermodynamic entropy production [3,4,5], there is considerable interest in their accurate characterization. The simplest way to visualize the local and global (time-averaged) Lyapunov exponents is to imagine the deformation of an infinitesimal j -dimensional volume \otimes_j in N -body phase space. The phase-space volumes $\{\otimes_j\}$ are all “comoving,” centered on an evolving trajectory that obeys the usual equations of motion. The instantaneous and the time-averaged rates at which the volumes grow or decay,

$$\{\dot{\otimes}_j/\otimes_j\} \text{ and } \{\langle\dot{\otimes}_j/\otimes_j\rangle\},$$

define the *sums* of the first j local and global Lyapunov exponents,

$$\sum_{i=1}^j \lambda_i \equiv \dot{\otimes}_j/\otimes_j; \quad \sum_{i=1}^j \langle\lambda_i\rangle \equiv \langle\dot{\otimes}_j/\otimes_j\rangle.$$

For instance λ_1 describes the instantaneous stretching (or shrinking) rate of a *line* joining two nearby trajectories; $\langle\lambda_1\rangle$ is the long-time-averaged value of this quantity; $\lambda_1 + \lambda_2$ describes the growth (or decay) rate of an *area* defined by three nearby trajectories, etc. Note that the local Lyapunov exponents are well defined point functions in phase space.

It is apparent that the local growth rates, $\sum_i \lambda_{i \leq j} \equiv \dot{\otimes}_j/\otimes_j$ depend on the *orientations* of the corresponding j -dimensional volumes in N -body phase space. Because the *initial* choice of such volumes is arbitrary it might appear that the local growth rates are ill defined. But after a “convergence time” τ —which we define and determine in the

present work—the initial choice becomes irrelevant, and the results for different choices all come to agree at sufficiently long times. The detailed time dependence of the convergence to unique orientations can be described by correlation functions defined and characterized in the work that follows. The time-dependent “converged orientation” of the volume \otimes_j has to be found by following the evolution of $j+1$ neighboring trajectories for a sufficiently long convergence time.

One might expect—naïvely as it turns out—that \otimes_1 , for instance, will turn into the direction of the fastest growth exponentially fast as

$$e^{-t/\tau}; \quad \tau \approx 1/\lambda_1.$$

Instead, we are able to argue, and confirm, that correlations appear at a rate determined by the *difference* of the first two Lyapunov exponents, $\lambda_1 - \lambda_2$. The directional error in δ_1 decays roughly as $1 - e^{-\Delta\lambda t}$ where $\Delta\lambda = \lambda_1 - \lambda_2$. We explore and evaluate possible generalizations of this idea to the remainder of the spectrum. We find, in fact, that the detailed convergence of the orientations is a relatively slow, and highly number-dependent ($\tau \propto N^p$), collective phenomenon.

For N -body systems with continuous force laws, such as the soft disks and soft spheres described in Sec. II, numerical investigations of Lyapunov spectra require computational work of order N^3 or N^4 per time step, with the power law depending on the chosen algorithm. The first numerical method to be discovered [6,7], with work $\propto N^3$, is still the one most commonly used. It relies on frequently repeated Gram-Schmidt orthonormalizations in the phase space. These orthonormalizations rescale, rotate, and orthogonalize a set of offset vectors that link a “reference” trajectory to nearby “satellite” trajectories. Together, these satellite trajectories span a small phase-space neighborhood of the reference trajectory.

Hoover and co-workers discovered an elegant Lagrange multiplier method [3,4,8] that prevents the growth or decay of the offset vectors $\{\delta_j\}$ while automatically incorporating the proper rotations of these vectors to maintain their orthogonality. The Lagrange multiplier method corresponds to a *continuous* (rather than frequently repeated) orthonormalization applied as a constraint on, rather than a correction to, the Hamiltonian motion of the j satellite trajectories, which define δ vectors spanning the hypervolume \otimes_j . This constraint method, combined with additional small-scale Gram-Schmidt orthonormalizations (to alleviate the small remaining errors due to computer roundoff) provides the best possible means for an accurate computation of the spectrum. The Lagrange multiplier method consumes computer time proportional to N^4 . Despite the disadvantage of increased computer time, we adopt this method here in order to optimize the *accuracy* of our results for continuous soft-disk and soft-sphere systems.

Hard disks and spheres, for which the main contributions to the Lyapunov exponents are singular ones, occurring at each successive two-body collision, require special methods [9–11]. Without taking special precautions, such as neighbor or cell lists, the computational cost of integrating a single trajectory for particles with hard elastic collisions scales as N^2 . In addition, the calculation of Lyapunov spectra requires the integration of the equations of motion of a complete set of infinitesimal displacement vectors δ_i .

Because in D dimensions each of these vectors has $2DN$ components and the total number of collisions per unit time is proportional to N , the CPU time required to follow the dynamics of all $2DN$ δ vectors is of order N^3 . The number of operations required to carry out a Gram-Schmidt orthonormalization is of the same order. In a typical calculation of a Lyapunov spectrum for a hard-particle system approximately equal amounts of CPU time are expended for Gram-Schmidt orthogonalization and propagation of all δ vectors. In general, the integration of a hard-sphere trajectory can be carried out with considerably higher efficiency than a trajectory for a system with continuous interactions. When, however, Gram-Schmidt orthonormalization becomes the dominant factor, the computational effort required for the calculation of Lyapunov spectra in systems of hard and soft spheres is of the same order.

We apply the Lagrange multiplier method here to many-body systems of soft disks and spheres in a dense-fluid thermodynamic state. We establish the rates of convergence of the local exponents and their corresponding δ vectors. The soft-particle systems chosen for investigation are described in Sec. II. We carry out analogous simulations for systems of hard disks and hard spheres. These hard-particle systems are described in Sec. III. Calculations for both the soft and the hard particles, followed by our conclusions, based on comparing them, make up the balance of this work.

II. SOFT-DISK ($D=2$) AND SOFT-SPHERE ($D=3$) MANY-BODY SYSTEMS

We continue here our study of square parallel systems of soft-disk fluid [12–15]. In all these systems any two disks

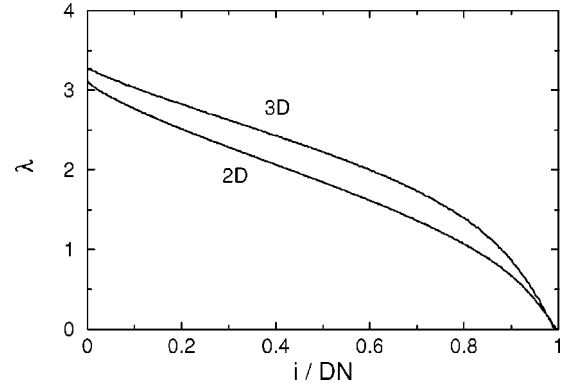


FIG. 1. Spectrum of time-averaged Lyapunov exponents for 256 soft disks (the data for 1024 show no noticeable differences) and for 125 soft spheres. In both cases the largest $DN-D-1$ of the $2DN-2D-2$ nonvanishing exponents are shown.

separated by less than unit distance interact with each other according to the short-ranged pair potential,

$$\phi(r < 1) = 100(1 - r^2)^4; \quad \Phi = \sum_{i < j} \phi(r_{ij}).$$

In three dimensions we use cubic systems, with exactly the same pair potential and with periodic boundary conditions. In both two and three dimensions we vary the total number of particles N , keeping the number density, the mass per particle, and the total energy per particle all equal to unity. Thus the soft-particle systems studied here all correspond to dense fluids.

In the two-dimensional thermodynamic equilibrium state the time-averaged potential energy is about 30% of the total energy $E = \Phi + K$,

$$\langle \Phi/N \rangle \approx 0.30; \quad \left\langle \frac{K}{N} \right\rangle = \left\langle \frac{p^2}{2m} \right\rangle \approx 0.70.$$

In three dimensions the potential energy is about 25% of the total. An effective hard-particle collision diameter σ for the soft particles can be estimated by considering the line-of-centers turning-point energy, $2kT$ for a typical thermal collision,

$$\phi(\sigma) = 2kT = \left(\frac{2K}{N} \right) \rightarrow \sigma_{D=2} = 0.810 \left(\frac{V}{N} \right)^{1/2};$$

$$\phi(\sigma) = 2kT = \left(\frac{4K}{3N} \right) \rightarrow \sigma_{D=3} = 0.827 \left(\frac{V}{N} \right)^{1/3}.$$

Apart from $2D+2$ vanishing coefficients, which correspond to constants of the motion [8,14], the long-time-averaged Lyapunov spectrum for the soft-disk equilibrium state is a well-known featureless continuous curve, illustrated in Fig. 1. The soft-sphere spectrum—a sample is shown in the same figure—is very similar. The largest of the $2ND-(2D+2)$ nonvanishing Lyapunov exponents, $\langle \lambda_1 \rangle$, defines an effective “collision rate” or “bifurcation rate” for these systems.

For all the two- or three-dimensional soft-particle systems we use the classic fourth-order Runge-Kutta integration [3,4,16] algorithm. For the work described here, accurate results are obtained with a time step $dt=0.002$. The resulting single-step integration error for sufficiently smooth solutions is of order $dt^5/5! \approx 10^{-15}$, about the same as the computational roundoff error. Such precise convergence can be easily spoiled by force functions with low-order discontinuous derivatives. Consider, for example, the Weeks-Chandler-Andersen potential, with forces that vanish *linearly* at the potential cutoff. Integrating the differential equation for the momentum p , $\dot{p}=F$, for a time step during which the interparticle force $F(r \approx 1)$ enters (or leaves) the interaction region, incurs a coordinate error of order $F[r=1 - (pdt/m)]dt^2/m \propto dt^3$ rather than dt^5 . In the present work we use forces that incur force errors that are *cubic* in (pdt/m) , with corresponding coordinate errors that *quintic* in dt . Thus our errors from force-law singularities do not exceed the inherent Runge-Kutta numerical errors, which are themselves at the level of computational roundoff errors.

III. HARD-DISK ($D=2$) AND HARD-SPHERE ($D=3$) MANY-BODY SYSTEMS

In all our systems with impulsive disk or sphere elastic collisions time is measured in units of $(m\sigma^2N/K)^{1/2}$, where m is the particle mass (unity for convenience), σ is the particle diameter, and $E=K$ is the total (kinetic) energy of the system. Periodic boundary conditions apply. The only relevant parameter is the density $\rho \equiv Nm/V = N/V$, where V is the volume (area, in two dimensions) of the simulation box. For our hard-disk simulations we use a box with an aspect ratio of $2/\sqrt{3}$ commensurate with the lattice structure at close packing. In three dimensions our simulation box is cubic. All simulations are carried out at densities corresponding to a dense fluid.

For the calculation of full Lyapunov spectra, the time evolution of a complete set of δ vectors must be determined. Between collisions, the smooth evolution of the δ vectors can be calculated analytically. The vectors change abruptly at collisions. Appropriate collision rules for the evolution of the δ vectors in tangent space can be derived from a collisional approximation which is linear in both the time and the phase-space coordinates [9]. Periodically the system of δ vectors is orthonormalized and the Lyapunov exponents are obtained as time averages of the growth rates of the δ vectors. The largest Lyapunov exponent, for instance, can be written as

$$\lambda_1 = \frac{1}{nt_w} \sum_{i=1}^n \ln s_1(t_i, t_w) \equiv \langle \lambda_1(t, t_w) \rangle,$$

where $s_1(t_i, t_w)$ is the length of delta vector δ_1 just before the i th orthonormalization, t_w is the time *window* between orthonormalizations and nt_w is the total simulation time. The above equation defines a “local” Lyapunov exponent $\lambda_1(t, t_w) \equiv \ln s_1(t, t_w)/t_w$ averaged over time t_w . While the fluctuations $\langle (\lambda - \langle \lambda \rangle)^2 \rangle$ of the local Lyapunov exponents

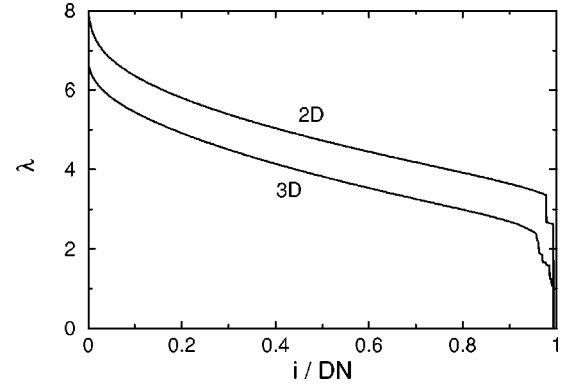


FIG. 2. Spectrum of time-averaged Lyapunov exponents for 256 hard disks and 256 hard spheres. In both these cases the largest $DN-D-1$ of the $2DN-2D-2$ nonvanishing exponents are shown.

are well defined for systems with smooth interactions, the fluctuations $\langle (\lambda(t, t_w) - \langle \lambda \rangle)^2 \rangle$ diverge, as $1/t_w$, as the window time t_w approaches 0.

The most positive halves of Lyapunov spectra for hard disks ($D=2$) and hard spheres ($D=3$) appear in Fig. 2. Both numerical [10] and theoretical [11] results indicate that for $N \rightarrow \infty$ Lyapunov spectra converge towards a finite thermodynamic limit. The conspicuous gap between zero and the first nonvanishing Lyapunov exponent, which is absent in systems with smooth interactions, vanishes in the limit $N \rightarrow \infty$ yielding a spectrum approaching zero with infinite slope [17].

IV. CALCULATIONS AND RESULTS

The phase space for all of our N -body D -dimensional systems is $2ND$ dimensional so that the complete Lyapunov spectrum consists of ND “pairs” of exponents $\pm \lambda$. The ND pairing relations,

$$\langle \lambda_j + \lambda_{2ND+1-j} \rangle \equiv 0,$$

are consequences of the underlying time-reversible Hamiltonian mechanics.

One might expect that the largest Lyapunov exponent, λ_1 , would converge, very roughly speaking, with an error of order $e^{-\langle \lambda_1 \rangle t}$. The second-largest exponent would likewise converge, but more slowly, with an error of order $e^{-\langle \lambda_2 \rangle t}$, if its convergence is essentially independent of the larger exponent $\langle \lambda_1 \rangle$. Alternatively, the second exponent might have to wait for the convergence of the first, leading to a longer estimate for the convergence time,

$$\tau \approx (1/\langle \lambda_1 \rangle) + (1/\langle \lambda_2 \rangle).$$

For a spectrum that approaches zero smoothly, as do the spectra for soft disks and spheres, this latter point of view suggests, evidently correctly, a *divergent* time for convergence as the system size increases. It is a major focus of the present work to determine how the convergence times and fluctuations of the Lyapunov exponents vary with the index j and the number of particles N .

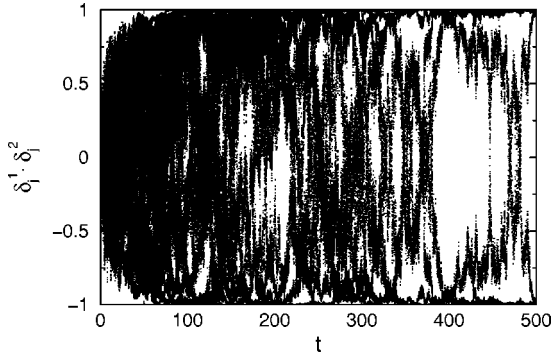


FIG. 3. Time evolution of $\{\delta_j^1 \cdot \delta_j^2\}$ for 64 soft disks. The dot products link corresponding members of two sets of 32 orthogonal vectors, $1 \leq j \leq 32$ initially chosen randomly. Completely uncorrelated orthogonal vectors correspond to a vanishing dot product while completely converged dot products have either of the values ± 1 .

There are many ways, different in detail, to assess the convergence rates of δ_1 or of the entire spectrum. A glimpse of the complexity such assessments could describe can be gleaned from Fig. 3, which shows a typical time development of 32 δ -vector dot products. The vectors chosen for the computation come from the two independent orthogonal sets “1” and “2.” Corresponding vectors (those describing the same Lyapunov exponent, one from each set) are multiplied: $\{\delta_j^1 \cdot \delta_j^2\}$. The dot products shown in the figure correspond to the 32 largest Lyapunov exponents in a 64-disk system. Notice that the time required for the first dot product $\delta_1^1 \cdot \delta_1^2$ to reach unity is of order 90 for a 64-particle system, *many* orders of magnitude larger than the straightforward guess $0.3 \approx 1/\langle \lambda_1 \rangle$.

A. Convergence times

The long times required for convergence of the full set of vectors suggest a more modest goal—quantifying the convergence of the vector associated with the largest Lyapunov exponent. This problem is feasible for system sizes up to about 1000 particles. Because convergence depends on the initial conditions, it is evident that some *averaging* procedure must be part of any accurate assessment of the number dependence. Here we average by first choosing 16 orthogonal phase-space vectors, $\{\delta_1^1, \dots, \delta_1^{16}\}$. We then follow the sum S_{dot} of all their dot products,

$$S_{\text{dot}} \equiv \frac{2}{15 \times 16} \sum_{i=1}^{15} \sum_{j=i+1}^{16} \delta_1^i \cdot \delta_1^j,$$

in time. From the initial value zero, the sum will eventually increase to unity. We tabulate the time at which the sum first reaches half of that value, $\frac{1}{2}$, and repeat this process ten times to improve the statistics. The resulting relaxation or convergence times $\{\tau(N)\}$ are displayed in Fig. 4.

The convergence times vary sufficiently regularly as to suggest the form of the large-system behavior. See again Fig. 4. $\tau(N)$ increases strongly, but not quite linearly, with N . A rough description of these results is that the vectors converge

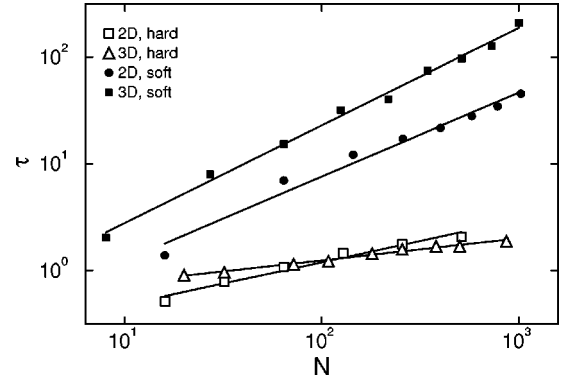


FIG. 4. Number dependence of the convergence of 16 orthogonal phase-space vectors. The time at which the sum first reaches half of its long-time value is plotted as a function of the number of particles N . The points correspond to systems of up to 1024 particles in two dimensions and 1000 particles in three dimensions. The filled symbols refer to soft-particle results and the empty symbols refer to hard-particle results. For the hard-particle results the densities were $\rho = 0.8\sigma^{-2}$ (disks) and $\rho = 0.85\sigma^{-2}$ (spheres). The convergence times grow as $N^{-\alpha}$, where $\alpha \sim 0.4$ (disks) and $\alpha \sim 0.2$ (spheres) for hard particles and $\alpha \sim 0.8$ (disks) and $\alpha \sim 0.9$ (spheres) for soft particles.

in a time of order N^α , where α lies between 0.2 (for hard spheres) and 0.9 (for soft ones). The time is significantly longer in three dimensions than in two (though the Lyapunov exponents are similar). In all cases, the convergence time increases with system size, as a *fractional* power somewhat less than unity.

In our preliminary exploratory *soft*-particle work we were surprised to find that the full sets of vectors fail to converge without specially matching the vectors corresponding to the constants of the motion. Evidently the differing curvatures—as well as differences in phase-space flow velocities—on the energy surfaces of the satellite trajectories, are responsible for differences in the local values of all the negative-exponent vectors. By imposing constraints identifying the corresponding δ vectors from the two sets, the curvature and velocity differences could be eliminated with the result that all the remaining δ vectors coincide in pairs at long times. The corresponding convergence times for the complete set of δ vectors are very similar to those found for the positive-exponent vectors alone or for the negative vec-

TABLE I. Soft-disk convergence times for the $2N-3$ positive Lyapunov exponents and the $2N-3$ negative Lyapunov exponents for independent sets of δ vectors. In calculating the negative exponents all the δ vectors for non-negative exponents were identical in the two sets. The data represent average convergence times for as many as 100 different sets of vectors.

N	$\langle \tau_+ \rangle$	$\langle \tau_- \rangle$
4	1.58	0.58
9	7.14	6.18
16	15.77	13.72
25	26.56	25.98

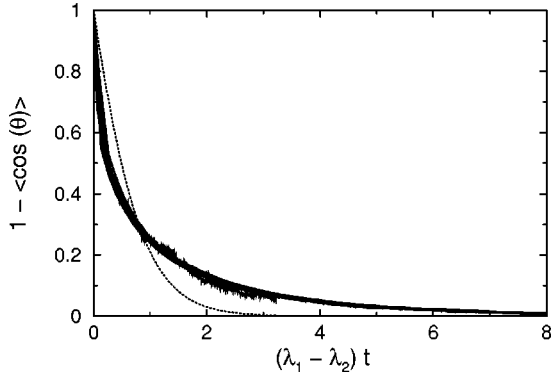


FIG. 5. Correlation functions $1 - \langle \cos(\theta) \rangle$ (see Sec. IV B) for initially random δ vectors as a function of $(\lambda_1 - \lambda_2)t$. The solid lines indicate results obtained for different particle numbers at various densities for hard and soft disks and spheres. The dotted line indicates the results of the simple theory presented in Sec. IV B. Rescaling time by the difference between the two largest Lyapunov exponents makes all the numerical curves essentially identical. The Lyapunov exponents required for such a rescaling were obtained in separate simulations.

tors along with the non-negative ones constrained to match. For example, soft-disk numerical values for these two choices are given in Table I. We found that hard-particle systems behave in a simpler way, with a pairing of exponents unaffected by the constants of the motion. Evidently the purely kinetic energy of hard particles simplifies the convergence.

B. Correlation function for δ vectors

The form of the correlation function describing the convergence of an arbitrary δ vector to the direction described by δ_1 can be estimated by ignoring the contributions of those Lyapunov exponents smaller than the largest two. If we use δ_{\parallel} and δ_{\perp} for the components of an arbitrary δ vector parallel and perpendicular to δ_1 , the equations of motion for the two kinds of components are

$$\dot{\delta}_{\parallel} = \lambda_1 \delta_{\parallel} - \lambda \delta_{\parallel}; \quad \dot{\delta}_{\perp} = \lambda_2 \delta_{\perp} - \lambda \delta_{\perp},$$

where the Lagrange multiplier λ maintains the total length $\delta_{\parallel}^2 + \delta_{\perp}^2 \equiv 1$,

$$\lambda \equiv \delta_{\parallel}^2 \lambda_1 + \delta_{\perp}^2 \lambda_2.$$

The time dependence of the dot product $\delta \cdot \delta_1 \equiv \cos(\theta)$ follows from the differential equation for the angle θ ,

$$\dot{\theta} = -\Delta\lambda \sin(\theta)\cos(\theta),$$

where $\Delta\lambda \equiv \lambda_1 - \lambda_2$. To solve the equation, note the identity,

$$(d/dt) \ln \tan(\theta) = \dot{\theta} / [\sin(\theta)\cos(\theta)].$$

Thus the $\dot{\theta}$ equation has the simple solution

$$\tan(\theta) = \tan(\theta_0) e^{-\Delta\lambda t}.$$

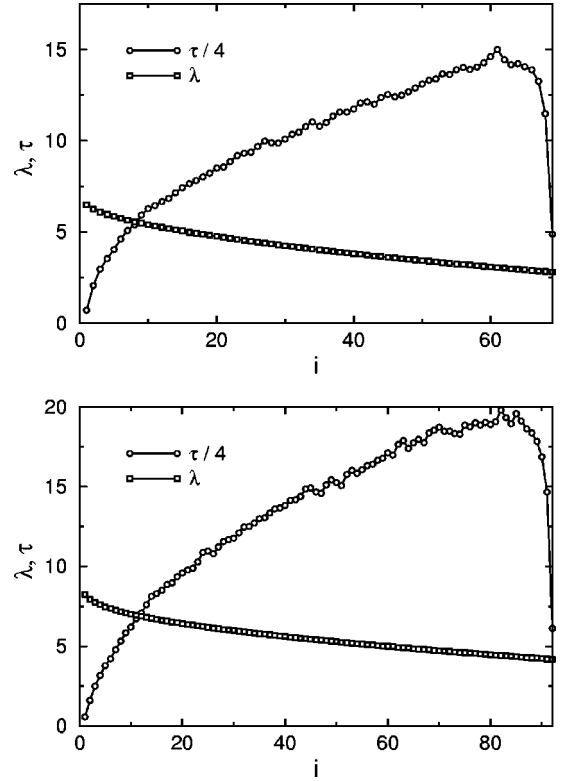


FIG. 6. Lyapunov spectra and corresponding convergence times for $N=36$ hard disks (top panel) and $N=32$ hard spheres (bottom panel). The densities were $\rho=0.8\sigma^{-2}$ and $\rho=0.8\sigma^{-3}$, respectively, corresponding to a dense fluid in both cases. Only positive exponents and corresponding convergence times are shown. The relaxation times for conjugate pairs of exponents are identical.

Exactly this same differential equation (with this same solution) results from Moran and Hoover's analysis of the two-dimensional isokinetic Galton board problem [3]. The analogy between thermostated momenta and constrained δ vectors is in fact precisely what led Posch and Hoover to the Lagrange multiplier method discussed in Ref. [12].

The analytic result for the *dot-product correlation function*, $1 - \cos(\theta)$ is shown as the dotted line in Fig. 5. The dot-product correlation functions obtained numerically for hard spheres and hard disks at various densities and particle numbers are shown as a heavy line, the superposition of all the separate data. The simple analytical result reproduces the convergence time approximately, but clearly differs in shape from the numerical results.

It is remarkable that scaling of time by $1/\Delta\lambda$ yields essentially identical curves for all conditions. This result indicates that the difference $\Delta\lambda$ between the largest and the second-largest exponent determines the time required for the relaxation of δ vectors, as predicted by the simple considerations presented above. The curves shown in Fig. 5 can be described quite well with either of two analytic approximations,

$$f(x) = a/(b + e^{cx}),$$

$$f(x) = ae^{-bx} + ce^{-4bx},$$

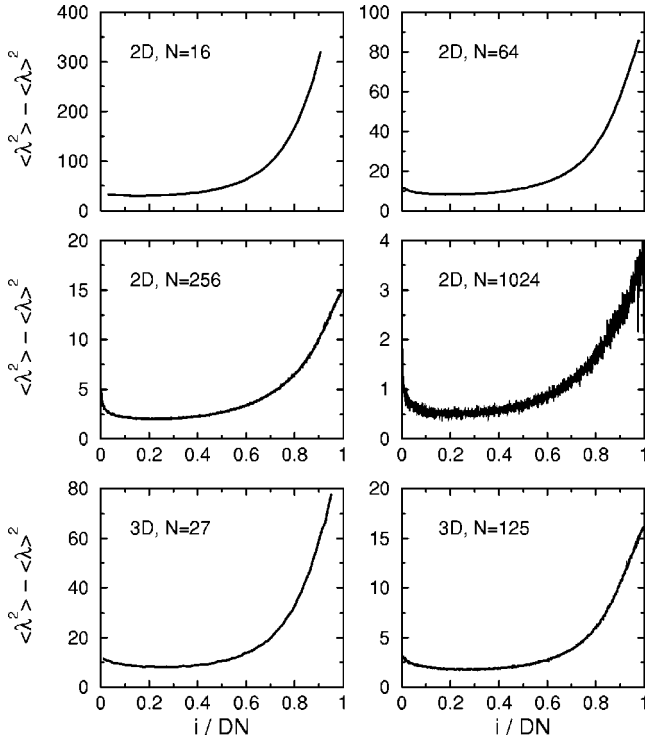


FIG. 7. Mean square fluctuations of the Lyapunov exponents for 16, 64, 256, and 1024 soft disks and for 27 and 125 soft spheres. Fluctuations for the negative exponents are identical to those for the positive exponents shown here.

where x is a dimensionless time, $x = \Delta \lambda t$. We have no theoretical justification for either form. Relaxation times for complete sets of hard-disk and hard-sphere δ vectors are plotted in Fig. 6, along with their corresponding Lyapunov exponents.

C. Number dependence of $\langle \lambda_1 \rangle$ and its fluctuation

For the soft particles, we have also computed the mean values and the *fluctuations* in the local Lyapunov exponents by computing corresponding long-time averages:

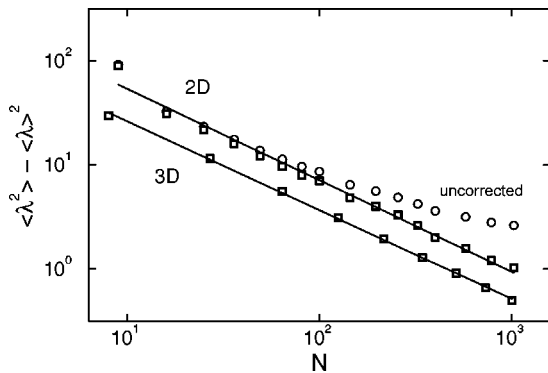


FIG. 8. Mean square fluctuations of the largest Lyapunov exponent for series of soft-disk and soft-sphere systems. The curvature in the two-dimensional fluctuations can be removed by subtracting a constant. This indicates that the two-dimensional fluctuations do not vanish in the large-system limit.

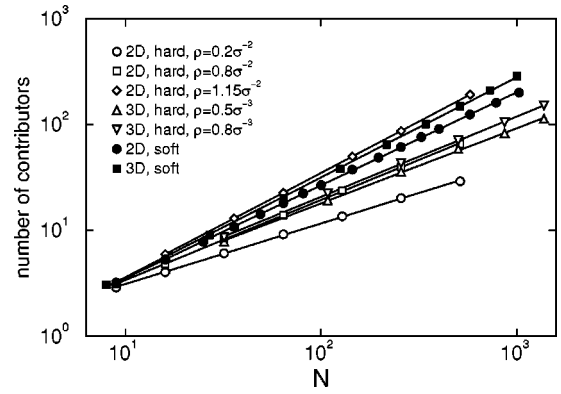


FIG. 9. Number of particles contributing to δ_1 by more than the average as a function of particle number N for a variety of different systems. The straight lines fitted to the data indicate that the number of contributors increases as a power of the number of particles with exponents in the range from 0.57 to 0.97.

$$\langle \lambda_j \rangle \equiv \frac{1}{t} \int_0^t \lambda_j(t') dt'; \quad \langle \lambda_j^2 \rangle \equiv \frac{1}{t} \int_0^t \lambda_j^2(t') dt'.$$

Our goal here is to characterize the variation of these fluctuations with the exponent index j . See Fig. 2 for the time-averaged spectra and Fig. 7 for the fluctuations. The data indicate power-law dependences of the spectra, as is described in more detail below.

For simplicity we confine our analysis here to the largest Lyapunov exponent λ_1 , and its fluctuation,

$$\mathcal{F} \equiv \langle (\lambda_1 - \langle \lambda_1 \rangle)^2 \rangle.$$

In both two and three dimensions these fluctuations converge much more rapidly than does the dot-product correlation function discussed in Sec. IV B.

The log-log plot in Fig. 8 shows fluctuations for $N = 4^2, 8^2, 12^2, \dots, 32^2$ particles in two dimensions and $N = 2^3, 3^3, 4^3, \dots, 10^3$ in three dimensions. The three-dimensional data indicate that the fluctuations vanish as $N^{-0.86}$ while the two-dimensional data show a considerable curvature. This curvature indicates a *residual fluctuation* in λ_1 , which persists in the large-system limit in two dimensions. If a constant is subtracted from the two-dimensional fluctuations, the data then become consistent with the power-law relation:

$$(\mathcal{F} - 1.6) \propto N^{-0.84}.$$

Similar persistence of fluctuations of local exponents has been recently observed in one-dimensional lattices of coupled logistics maps [18].

D. Number dependence of contributors to δ_1

The maximum Lyapunov exponent has been observed to be correlated with spatially localized trajectory perturbations [13]. To investigate this localization phenomenon further, we computed the number of particles contributing to δ_1 , the δ

vector associated with the largest Lyapunov exponent. More precisely, we have determined the number of particles for which the i th contribution

$$C_i \equiv \delta x_i^2 + \delta y_i^2 + \delta p_{x,i}^2 + \delta p_{y,i}^2$$

is larger than the average value $1/N$. In all cases we have found that the average number of such particles grows more slowly than linearly, indicating that, in the limit $N \rightarrow \infty$, a vanishing fraction of the particles contributes to δ_1 . This is quite consistent with existing results for hard disk and dumbbell systems [19]. As shown in Fig. 9 for a variety of soft and hard-particle systems, the number of contributors grows as N^α , where the exponent α depends on the dimensionality, the form of the interaction potential, and the thermodynamic state.

V. CONCLUSIONS

The local Lyapunov exponents, as well as their fluctuations, converge relatively rapidly to simple featureless curves. The number dependence of the exponents, and their fluctuations, the relaxation times, and the number of particles associated with particular δ vectors, all follow simple power laws. The precise alignment of the δ vectors that define these

exponents is slow to converge, as might be expected for a collective phenomenon linking all the particles in a many-body system.

So far very little is known about the mechanisms governing convergence. Existing theoretical efforts [20,21] point out possible approaches, but have so far been unable to distinguish the dependence of Lyapunov spectra on (i) phase, (ii) dimensionality, and (iii) strength of the pair potential. It is very gratifying that a single universal form appears to describe both the soft and the hard-particle correlations, both in two dimensions and in three dimensions.

ACKNOWLEDGMENTS

C.D.'s work at Rochester was supported by a grant from the donors of the Petroleum Research Fund, administered by the American Chemical Society. W.G.H.'s work in Carol Hoover's Methods Development Group at the Lawrence Livermore National Laboratory was performed under the auspices of the United States Department of Energy through University of California Contract No. W-7405-Eng-48. H.A.P.'s work at Vienna was supported by a grant from the Fonds zur Förderung der wissenschaftlichen Forschung, Grant No. P15348-PHY.

-
- [1] W. G. Hoover, C. G. Hoover, and H. A. Posch, *Phys. Rev. A* **41**, 2999 (1990).
 - [2] G. Paladin and A. Vulpiani, *Phys. Rep.* **156**, 147 (1987).
 - [3] W. G. Hoover, *Computational Statistical Mechanics* (Elsevier, New York, 1991).
 - [4] W. G. Hoover, *Time Reversibility, Computer Simulation, and Chaos* (World Scientific, Singapore, 1999).
 - [5] K. Aoki and D. Kusnezov, e-print nlin. CD/0204015 (2002).
 - [6] G. Benettin, L. Galgani, A. Giorgilli, and J. M. Strelcyn, *Mechanica* **15**, 9 (1980).
 - [7] I. Shimada and t. Nagashima, *Prog. Theor. Phys.* **61**, 1605 (1979).
 - [8] W. G. Hoover, H. A. Posch, and S. Bestiale, *J. Chem. Phys.* **87**, 6665 (1987).
 - [9] C. Dellago, H. A. Posch, and W. G. Hoover, *Phys. Rev. E* **53**, 1485 (1996).
 - [10] C. Dellago and H. A. Posch, *Physica A* **250**, 68 (1997).
 - [11] R. van Zon, H. van Beijeren, and C. Dellago, *Phys. Rev. Lett.* **80**, 2035 (1998).
 - [12] W. G. Hoover, *Phys. Rev. A* **37**, 252 (1988).
 - [13] W. G. Hoover, K. Boercker, and H. A. Posch, *Phys. Rev. E* **57**, 3911 (1998).
 - [14] H. A. Posch and W. G. Hoover, *Phys. Rev. A* **39**, 2175 (1989).
 - [15] W. G. Hoover, H. A. Posch, C. Forster, Ch. Dellago, and M. Zhou, *J. Stat. Phys.* (to be published).
 - [16] F. J. Vesely, *Computational Physics—An Introduction*, 2nd ed. (Plenum, New York, 2001).
 - [17] Lj. Milanović, Ph.D. thesis, University of Wien, 2001.
 - [18] A. Pikovsky and A. Politi, *Nonlinearity* **11**, 1049 (1998).
 - [19] Lj. Milanović and H. A. Posch, *J. Mole. Liq.* **96-97**, 221 (2002).
 - [20] S. McNamara and M. Mareschal, *Phys. Rev. E* **64**, 051103 (2001).
 - [21] J. P. Eckmann and O. Gat, *J. Stat. Phys.* **98**, 775 (2000).